THE JOURNAL OF PHYSICAL CHEMISTRY B

Article

pubs.acs.org/JPCB

An Optical Microscopy Study on the Phase Structure of Poly(L-lactide acid)/Poly(propylene carbonate) Blends

Min Gao, Zhongjie Ren, and Shouke Yan*

State Key Laboratory of Chemical Resource Engineering, Beijing University of Chemical Technology, Beijing 100029, China

Jingru Sun and Xuesi Chen

State Key Laboratory of Polymer Physics and Chemistry, Changchun Institute of Applied Chemistry, The Chinese Academy of Sciences, Changchun 130022, China

ABSTRACT: The dependence of phase structure of PLLA/PPC blends on the blend ratio, the heat-treatment temperature and time was investigated by optical microscopy. It is found that, at lower PPC content, e.g., less than 30%, the PLLA crystalline spherulites fill the whole space with the PPC dispersed in the amorphous region of PLLA. No evident phase separation has been observed under optical microscope. When the content of PPC reaches 40%, phase separation takes place. The phase separation of the PLLA/PPC blend happens prior to the crystallization of PLLA. Therefore, the heat-treatment temperature and time are the two most important factors that control the phase structure of the blend. At low heat-treatment temperatures, e.g., lower than 190 °C, the PPC and the amorphous PLLA part compose a continuous phase with the crystalline PLLA domains dispersed in it. When the sample was heat-treated at 200 °C for 5 min, a bicontinuous phase structure was observed. With further increase of the heat-treatment temperature, the crystalline PLLA composes the continuous phase with PPC domains randomly dispersed in it. Similar phase reversal phenomenon has also been observed by heat-treating the samples at 200 °C for different times. It is further confirmed that the crystallization of PLLA in the blends is influenced by the different phase structures. For example, the crystallinity of PLLA in the blend increases with increasing heat-treatment temperature.

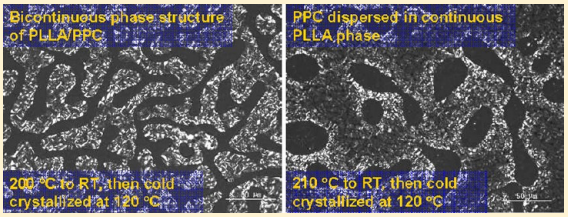

1. INTRODUCTION

Poly(L-lactic acid) (PLLA) has attracted more and more attention in recent years, since it is not only biodegradable at the ambient environment but also can be produced from the renewable biomass such as corn.[1−5] It has been extensively studied for application in the biomedical devices and biodegradable plastics because of its high strength, high modulus, and biocompatibility.[6,7] However, in many cases, the practical applications of PLLA have been significantly limited by its relatively high price, low heat distortion temperature, and inherent brittleness. Therefore, different chemical and physical approaches have been developed for improving these properties.[8−11] Chemical method for modifying the properties of PLLA has been most frequently realized by copolymerization to produce graft or block copolymers, such as poly(vinyl alcohol)-*g*-poly(L-lactic acid), polyurethane-*g*-poly(L-lactic acid), poly(L-lactic acid)-*b*-poly(oxpropylene-*co*-oxyethyene), and poly(L-lactic acid)-*b*- poly(oxypropylene)-*b*-poly(L-lactic acid).[12−15] For the physical approach, the most easy and efficient way is to blend the PLLA with different kinds of fillers or/and with other polymers of complementary property features, such as poly(ε-caprolactone) (PCL), poly(butylenes succinate) (PBS), and natural fiber flax.[16−18] In some cases, epitaxial crystallization may produce special oriented structure, which can further enhance the strength of the material with synergetic effect—as an example, the perpendicular arranged lamellar structure between PLLA and polyethylene.[19]

In this study, PLLA was blended with poly(propylene carbonate) (PPC) under the consideration of the following three points. First of all, PPC is also a biodegradable aliphatic polycarbonate. Due to the utilization of carbon dioxide (CO_2) as one of the reaction components, the synthesis of PPC exhausts CO_2.[20] Second, the chemical structures of PLLA and PPC are similar as shown in Figure 1; they are consequently expected to be miscible and compatible to some extent.[21] Third, considering that the PLLA presents good mechanical

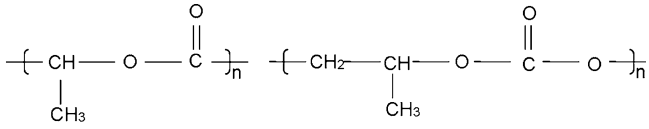

poly(l-lactic acid) (PLLA) poly(propylene carbonate) (PPC)

Figure 1. Chemical structures of PLLA and PPC.

Received: April 30, 2012
Revised: July 23, 2012
Published: July 24, 2012

   dx.doi.org/10.1021/jp3041378 | *J. Phys. Chem. B* 2012, 116, 9832−9837

properties but poor elasticity, while PPC exhibits good elasticity but poor mechanical strength,[22−24] the PPC in the PLLA-rich blends can toughen the PLLA, while the PLLA in the PPC-rich blends is expected to reinforce the PPC on the other hand.

It is well-known that the properties, sometimes even the functionalities, of a polymeric material depend strongly on its morphology and structure in the condensed state. For example, the electrical conductivity of well-aligned conjugated macromolecules can be increased more than a factor of 100 compared with their nonoriented counterparts.[25,26] Moreover, the poly(vinylidene fluoride) (PVDF) can only be used as general thermoplastics when in its α-form composed of helical chains, while its β-form with planar zigzag chains exhibits exceptional piezo- and pyroelectric properties.[27] For multiphase and multicomponent polymeric systems, the properties are also influenced significantly by the phase structure of the blends. As examples, while the phase structure of the donor and acceptor materials of polymer solar cells influence the efficiency of the device significantly,[28] the thermal stability of a polymer dispersed in a polymeric matrix depends remarkably on its domain size.[29] Moreover, different phase structure may in turn influence the crystallization behavior and the resultant crystal structure of the crystallizable component, as the PLLA used in this study. Therefore, understanding the phase separation behavior of a polymer blend is of great importance for tailoring the phase structure of the system, and consequently the properties of the polymer blend. Under this consideration, the dependence of phase structures of PLLA-rich PLLA/PPC blends on the composition and processing condition was investigated by optical microscopy. Also the effect of phase structure on the crystallization of PLLA in the PLLA/PPC blends was studied through crystallinity measurement by DSC.

2. EXPERIMENTAL DETAILS

Commercial grade poly(lactide) (PLA), Revode213H, with weight-average molecular weight (M_w) = 6.5 × 10^5 g mol^{-1} and polydispersity of 2.1 was obtained from Zhejiang Hisun Bimaterials co., Ltd. The glass transition temperature of it was estimated by DSC as 60 °C. PPC sample was kindly provided by Key Laboratory of Polymer Ecomaterials, Changchun Institute of Applied Chemistry, Chinese Academy of Sciences. The samples were all dried in vacuum oven at 60 °C for 24 h. The PLLA/PPC blends with weight ratios of 100/0, 90/10, 70/30, and 60/40 were dissolved in chloroform to make a solution with concentration of 10 wt %. Thin films of the blends were then prepared by casting the solution on glass slides where the solvent was allowed to evaporate in a controlled air stream for 1 day. The thickness of the resultant film is about 5 μm, which can be directly used for optical microscopy observation.

The morphologies of the PLLA/PPC blends with different blend ratios prepared under different conditions were observed with an optical microscope (Carl Zeiss Axioskop 40 A pol) under crossed polarizers. The optical microscope is equipped with a temperature controller (Linkam THMS600/CI94) with temperature accuracy of ±0.1 °C. To study the influence of crystallization temperature on the phase structure of the PLLA/PPC blends, the samples were heated to 200 °C for 5 min to erase the thermal history of the sample completely and then cooled at a rate of 100 °C/min to desired temperatures, ranging from 115 to 130 °C, for isothermal crystallization. To identify the effect of PLLA crystallization process on the phase separation behavior of the blends, the samples were quenched from different temperatures to room temperature, avoiding the crystallization of PLLA, and then cold-crystallized at different temperatures for sufficient time. In this way, crystallization-induced phase separation could be prevented. The effect of heat-treatment temperature on the phase separation behavior of the blends was studied by heating the samples to different temperatures ranging from 170 to 230 °C for 5 min before quenching to room temperature and then cold-crystallized isothermally at 120 °C for 4 h.

The crystallinity of PLLA in the PLLA/PPC blends with different phase structure was estimated by DSC experiments. To this purpose, a Perkin-Elmer differential scanning calorimeter (DSC-7) under nitrogen gas was used in this work. The temperature and the heat flow of the equipment were calibrated with indium and zinc. Samples of about 4−6 mg in weight were heated to 200 °C at a rate of 20 °C/min. The crystallinity of the PLLA, Φ_c, was calculated by the following equation

$$\Phi_c = \frac{\delta H_f}{W^{PLA} \times \delta H_f^0} \times 100\%$$

where δH_f^0 is the enthalpy of fully crystallized pure PLLA, which is 93.6 J·g^{-1} as reported in ref 30. δH_f is the enthalpy of PLLA crystallized in the blend, which is obtained from the peak area of the DSC curve. W^{PLA} is the weight ratio of PLLA.

3. RESULTS AND DISCUSSION

PLLA is a semicrystalline polymer with a very slow crystallization rate. Under normal cooling process, e.g., 10 °C/min, melt crystallization of PLLA does not occur. Therefore, the melt crystallization of PLLA is usually performed isothermally at elevated temperatures. Moreover, it is well documented that PLLA exhibits pronounced polymorphisms and morphologies depending on the thermomechanical treatments.[31−33] It was reported that the PLLA crystallizes from the melt at temperatures higher than 100 °C in the α-form with 10_3 left-handed helices packed in an orthorhombic unit cell,[31,34] even though the morphologies can be different according to the crystallization temperatures. Taking all these into account, we have first melt-crystallized the PLLA in its PLLA/PPC blends isothermally at 120 °C. Figure 2 shows the

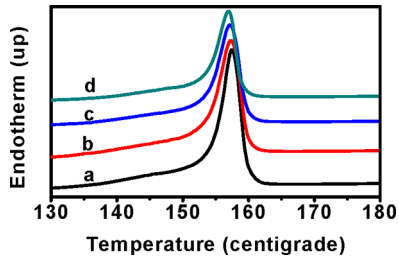

Figure 2. DSC heating scans of PLLA/PPC blends with different blend ratios crystallized isothermally at 120 °C for 15 h. The blend ratios are (a) 100/0; (b) 90/10; (c) 70/30; and (d) 60/40.

DSC heating scans of PLLA/PPC blends with different blend ratios prepared by isothermal crystallization at 120 °C for 15 h. The characteristic data including melting temperatures and fusion enthalpies as well as the crystallinities are listed in Table 1. From Figure 2, we can see that all of the samples show an endothermic peak at around 157 °C. With increasing PPC content, the melting point of the PLLA shifts only a little bit to

dx.doi.org/10.1021/jp3041378 | J. Phys. Chem. B 2012, 116, 9832−9837

Table 1. Characteristic Data of PLLA/PPC Blends with Different Blend Ratios Heat-Treated at 200 °C for 5 min and Then Melt-Crystallized Isothermally at 120 °C for 15 h

blend ratio PLLA/PPC	melt temp T_m (°C)	fusion enthalpy H_m (J/g)	crystallinity Φc (%)
100/0	157.46	53.08	56.7
90/10	157.31	51.91	61.6
70/30	157.16	41.59	63.5
60/40	156.93	32.87	58.5

the lower temperature, while the crystallinity of the blends increases first and then decreases evidently (see Table 1). The different crystallization behavior of the PLLA in the blends may be related to the composition-dependent phase structure of the blends. Therefore, the phase structure of the PLLA/PPC blends was studied in detail.

Presented first in Figure 3 are representative optical micrograghs of pure PLLA crystallized at different temperatures

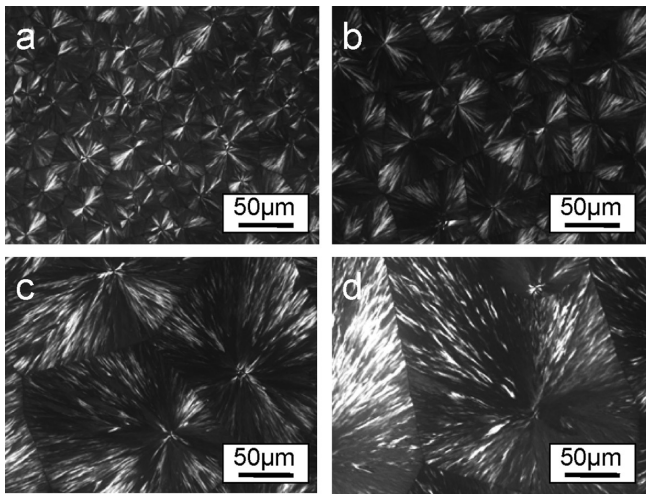

Figure 3. Optical micrographs of neat PLLA prepared by melting 5 min at 200 °C to erase the thermal history and then isothermally crystallized at (a) 115 °C, (b) 120 °C, (c) 125 °C, and (d) 130 °C for 8 h. The pictures were taken under crossed polarizers.

for a direct comparison. From Figure 3, we can see that the PLLA melt-crystallizes in the form of spherulites. The size of the PLLA spherulites increases with elevated crystallization temperature, while the number of the spherulites decreases evidently because of the reduced nucleation ability. At 130 °C (Figure 3d), the density of nucleus is very low. Therefore, we can observe only a few spherulites which grow to ca. 200 μm in diameter.

For polymer blends, composition of the blends is one of the most important factors that affects the phase structure of the system. For example, phase reversal can be generally produced according to the blend ratio. To study the influence of composition on the phase structure of PLLA/PPC blends, blends with PPC contents of 10%, 30%, and 40% were prepared. Figure 4 shows the representative morphologies of the resultant blends, which have been melted for 5 min at 200 °C and then crystallized isothermally at 120 °C for 4 h. From Figure 4, we see that blending PLLA with the amorphous PPC leads to an increase of the spherulite size of the PLLA; comparing Figure 4a,b with Figure 3b reveals that the spherulitic morphology of pure PLLA crystallized also at 120

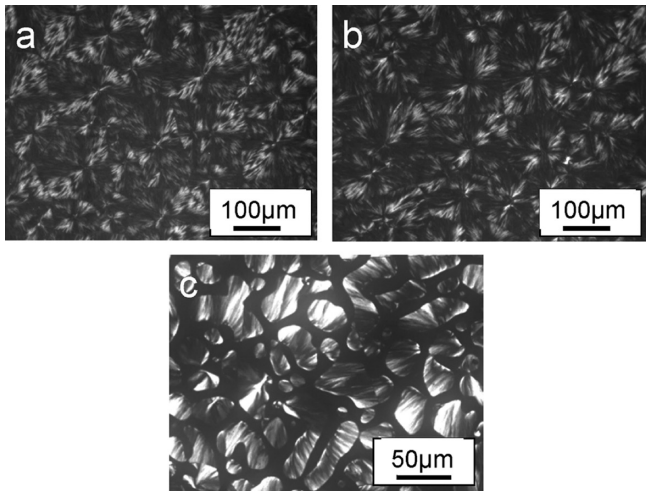

Figure 4. Optical micrographs of PLLA/PPC blends prepared by melting 5 min at 200 °C then isothermally crystallized at 120 °C for 4 h. The PLLA/PPC blend ratios are (a) 90/10, (b) 70/30, and (c) 60/40.

°C. For example, adding a 10% PPC into the PLLA results in a 3 or 4 times increase of the PLLA spherulites in diameter. Moreover, the PLLA spherulites are loosely packed with respect to the pure PLLA. Nevertheless, the PLLA spheruites form a continuous phase filling the whole view field when the PPC content is lower than 30% (see Figure 4b). In this case, the PPC is dispersed in the amorphous PLLA phase, or in other words, between the lamellae of PLLA. Taking the semicrystalline feature of polymers into account, the spherulitic structures shown in Figure 3a,b can be regarded as bicontinuous phase structure of crystalline PLLA and the amorphous PLLA together with the PPC. This may also indicate that PLLA and PPC are miscible and compatible to some extent as suggested by Ma et al.[21] Further increase of the PPC up to 40% (see Figure 3c) leads to an evident phase separation with the birefringent PLLA crystals not filling the whole field anymore. Now the discrete PLLA domains with strong birefringence are dispersed in a nonbirefringent amorphous matrix, which displays as typical sea-island structures. This seems hard to understand since PLLA is a majority component. It is acceptable when the low crystallinity of PLLA is considered. In this situation, the amorphous PPC together with the noncrystalline PLLA, which could be increased under the influence of PPC, leads to a high content of amorphous material and therefore compose a continuous amorphous matrix with the crystalline PLLA domains dispersed in it. From these observations, a conclusion may be drawn that, when the PPC content in PLLA/PPC blend increases up to 40%, the PLLA crystals form isolated phase randomly dispersed in the continuous amorphous matrix phase composed of both the PPC component and the amorphous PLLA portion. It should be pointed out that, except for the obvious phase separation shown in the optical micrograph of Figure 4c, the appearance of the PLLA is somewhat strange. Instead of apparent spherulitic structure, the birefringent parts shown in Figure 4c seem to be oriented or even as parts of a much larger superstructure. It may be explained in the following way. The occurrence of phase separation leads to the formation of PLLA-rich domains, which provides strong birefringence after crystallization. There is also a small amount of PLLA dispersed in the PPC-rich domains owing to some extent of miscibility. The PLLA

dx.doi.org/10.1021/jp3041378 | J. Phys. Chem. B 2012, 116, 9832−9837

dispersed in these domains may also crystallize during the isothermal process but shows no birefringence due to the limited amount of crystals. It is these crystals that connect the PLLA-rich domains and together form larger spherulites with the strong birefringent regions as parts of the big spherulite. The crystallization of PLLA in the PPC-rich domains of a 60/40 PLLA/PPC blend quenched from 230 °C and then cold-crystallized at 120 °C (see later Figure 7d) supports the above explanation.

The above experimental results clearly demonstrated the influence of blend ratio on the phase structure of PLLA/PPC blends. At low PPC content, the PLLA crystals fill the whole film sample with the PPC dispersed in it. When the PPC content reaches 40%, predominate PLLA crystals with strong birefringence form isolated domains inserted in the amorphous PPC matrix. This kind of phase structure can be produced either by crystallization of PLLA in the phase-separated domains or by crystallization-induced phase separation due to the exclusion of noncrystallizable materials into the crystal growth front, which blocks the propagation of the crystal and creates isolated crystal domains. Crystallization-induced phase separation happens even in the totally miscible blend systems since cocrystallization of the two components is generally impossible.[35−37] To find out whether the above-mentioned phase structure is the result of crystallization in separated phase or crystallization-induced phase separation, the influence of crystallization temperature on the phase structure of the 60/40 PLLA/PPC blend is followed. Figure 5 shows the optical

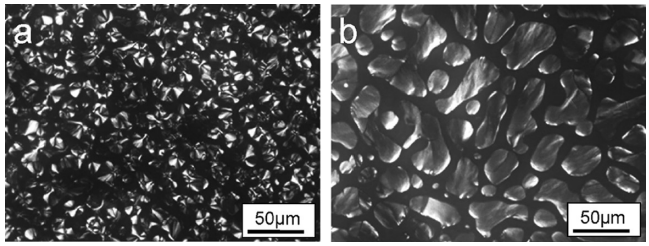

Figure 5. Optical micrographs of PLLA/PPC 60/40 blends prepared by melting 5 min at 200 °C and then isothermally crystallized at different temperatures: (a) 110 °C and (b) 135 °C.

micrographs of the 60/40 PLLA/PPC blends prepared by molten for 5 min at 200 °C and then crystallized isothermally at 110 and 135 °C, respectively. At first glance, one may find that the morphologies of the PLLA/PPC blends crystallized at 110 and 135 °C are totally different. For the sample crystallized at 110 °C (Figure 5a), small spherulites of ca. 30 μm in diameter can be recognized. On the other hand, the sample crystallized at 135 °C (Figure 5b) shows isolated domains with birefringence rather than spherulites. The sea-island structure formed at 135 °C has a close resemblance with that formed at 120 °C (compare Figure 5b with Figure 4c), while the PLLA crystals formed under 110 °C look more or less like a continuous phase. On close inspection, panels a and b of Figure 5 present actually a similar domain structure with the amorphous PPC as continuous phase inserted by PLLA crystalline domains. The difference should originate from the different nucleation ability of the PLLA at different crystallization temperatures. At 110 °C, the densely formed nuclei result in the formation of abundant small spherulites of the PLLA. At 135 °C, similar to the case at 120 °C shown in Figure 4c, the limited nuclei lead to the formation of big PLLA spherulites with strong birefringent PLLA-rich domains dispersed in them. This has been more clearly revealed by the morphologies of cold-crystallized samples.

Figure 6 shows the optical micrographs of the 60/40 PLLA/PPC blends first quenched from 200 °C to room temperature

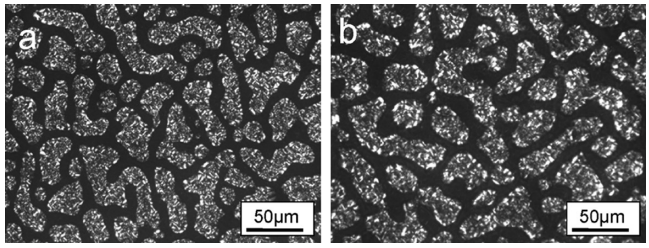

Figure 6. Optical micrographs of the 60/40 PLLA/PPC blends first quenched from 200 °C to room temperature to avoid crystallization of PLLA and then cold-crystallized isothermally at (a) 110 °C and (b) 135 °C, respectively.

to avoid the crystallization of PLLA and then cold-crystallized isothermally at 110 and 135 °C, respectively. Clearly, the cold-crystallized samples reveal a phase structure better than the melt-crystallized ones. The similar sea-island structures shown in Figure 6a,b indicate unambiguously that phase separation of the 60/40 PLLA/PPC blend takes place prior to the crystallization of PLLA. In other words, phase separation occurred during the heat treatment at 200 °C, which leads to the crystallization of PLLA mainly in the PLLA-rich domains during isothermal cold- or melt-crystallization processes. It should be pointed out here that the phase structures of the samples cold- and melt-crystallized both at 135 °C may be somewhat different from each other since phase separation can propagate further during the isothermal melt-crystallization process. This happens during melt crystallization at any temperature to different extents. Therefore, a slight domain size increment of the crystalline PLLA phase is seen when the isothermal melt-crystallization temperature changed from 110 to 135 °C. At the same time, the phase boundary gets smoother with elevated crystallization temperature—compare parts a and b of Figure 5.

The above experimental results clearly indicate that the phase separation of the PLLA/PPC blend is not induced by the crystallization of PLLA. It is formed already in the molten state before the crystallization of PLLA. This confirms that the composition-dependent crystallinity of the blends is the result of different phase structure. At low PPC content, no evident phase separation takes place. Therefore, the homogeneously dispersed PPC acts as solvent and enhances the crystallization ability of the PLLA. In this case, the crystallinity of the PLLA in the blends increases with increasing PPC content. When the content of the PPC reaches 40%, evident phase separation occurs. This reduces the solvent effect of the PPC toward PLLA and results in a decrease in crystallinity. Nevertheless, the crystallinity is still somewhat higher than the pure PLLA (see Table 1).

It should be pointed out that the heat-treatment temperature is a very important parameter that controls the phase structure of the blend system. The influence of the heat-treatment temperature on the phase structure of the 60/40 PLLA/PPC blend is illustrated in Figure 7. For clarity, samples first quenched from different temperatures and then cold-crystallized at 120 °C were used. From Figure 7, one can see that the

dx.doi.org/10.1021/jp3041378 | J. Phys. Chem. B 2012, 116, 9832−9837

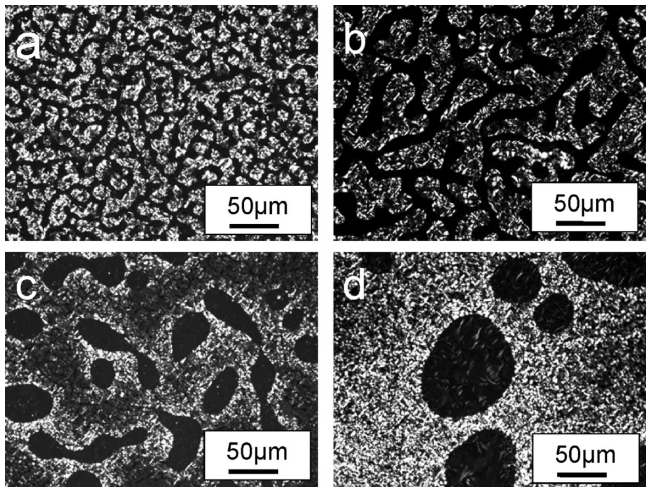

Figure 7. Optical micrographs of the 60/40 PLLA/PPC blends first quenched from different temperatures to room temperature and then cold-crystallized isothermally at 120 °C. The samples were heat-treated at (a) 190 °C, (b) 200 °C, (c) 210 °C, and (d) 230 °C for 5 min before quenching to room temperature and then cold-crystallized isothermally at 120 °C for 4 h.

phase structure of the blend depends strongly on the heat-treatment temperature. Under low melting temperature, e.g. 190 °C (Figure 7a), the blend exhibits essentially a continuous PPC phase with less connected PLLA crystalline domains dispersed in it. This results from the semicrystalline feature of polymers, which results in the existence of amorphous PLLA portion in the amorphous PPC domains. The phase separation gets severe with increasing heat-treatment temperature. For example, when the blend was quenched from 200 °C to room temperature (see Figure 7b) the sizes of the PLLA as well as the PPC domains get evidently bigger with respect to those shown in Figure 7a, indicating a higher extent of phase separation. Moreover, now the phase separation results in the formation of a bicontinuous phase structure. For the sample quenched from 210 °C, phase reversal takes place. As shown in Figure 7c, now the PPC component no longer forms a continuous phase but rather is dispersed randomly in the enriched PLLA matrix phase. With further increase of the heat-treatment temperature, e.g., 230 °C, regular round PPC domains of tens of micrometers dispersed in continuous PLLA matrix are observed, indicating a further evolution of the phase separation. It should be pointed out that weak birefringence can be identified in the PPC-rich domains. This means that the PLLA chains that remained in the PPC domains are also capable of crystallization. With close inspection, one can find that this happens already in the sample quenched from 210 °C, even though less pronounced. This can be explained in the following way. The prepared PLLA/PPC blends are initially well mixed. Phase separation takes place when they are heated over the melting temperature of PLLA owing to their poor miscibility. The separation kinetics depends on the temperature at which phase separation happens. At low temperature, the mobility of the molecular chains is poor, which leads to a short diffusion length. Therefore, the formed isolating domains of both components are smaller (Figure 7a). In this case, the crystallization of PLLA trapped in the amorphous PPC phase is suppressed. With increasing temperature, the chain mobility increased, leading to the formation of larger domains. At the same time, sufficient separation of PLLA chains from the PPC phase results in the crystallization of PLLA even in PPC-rich domains (Figure 7d). This may lead to an increment of the crystallinity of PLLA with increasing heat-treatment temperature. The DSC measurements confirmed that the crystallinity of PLLA in the 60/40 PLLA/PPC gets larger and larger with increasing heat-treatment temperature. As summarized in Table 2, the crystallinity of PLLA/PPC blend quenched from 170 °C and subsequently cold-crystallized at 120 °C is about 54%, while that of the sample quenched from 230 °C with unchanged crystallization temperature reaches 60%.

Table 2. Crystallinity of PLLA in the 60/40 PLLA/PPC Blends Heat-Treated at Different Temperatures for 5 min and Then Cold-Crystallized Isothermally at 120 °C for 4 h

heat-treatment temp/°C	crystallinity (Φ_c/%)
170	53.7
180	54.6
190	56.9
200	57.3
210	59.2
220	60.0

Another thing that should be addressed is the crystal size of the PLLA dispersed in the PPC-rich domains. From Figure 7d, with close inspection, one can find that the PLLA crystallized in the PPC-rich domains forms spherulitic structure with weak birefringence. These spherulites are clearly larger in diameter than those formed in the PLLA-enriched domains. This is related to the reduced nucleation ability of the PLLA dispersed in the PPC-rich domains.

The above results demonstrate that phase separation of PLLA/PPC blend takes place during the heat-treatment process. The phase structure depends remarkably on the heat-treatment temperature. With increasing heat-treatment temperature under otherwise unchanged conditions, phase reversal occurred for a 60/40 PLLA/PPC blend from continuous PPC phase to continuous PLLA phase. This is related to the increased molecular chain mobility. It should be pointed out that enhanced phase separation can also be achieved with prolonged time at fixed temperature. This has been well displayed in Figure 8, which shows the phase structure of the 60/40 PLLA/PPC blend heat-treated at 200 °C for different periods of time before quenching to room temperature and then cold-crystallized at 120 °C isothermally. Obviously, the phase structure of the sample heat-treated at 200 °C for 15 min is somewhat different from that of the sample heat-treated at 200 °C for 5 min; compare Figure 8a with

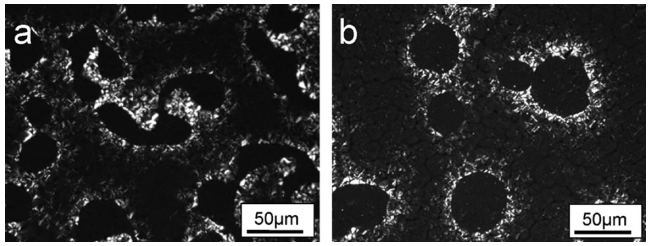

Figure 8. Optical micrographs of the PLLA/PPC 60/40 blends prepared by melting at 200 °C for (a) 15 min and (b) 20 min, quenched to room temperature and then cold crystallized isothermally at 120 °C.

dx.doi.org/10.1021/jp3041378 | J. Phys. Chem. B 2012, 116, 9832−9837

Figure 7b. Instead of a continuous PPC phase, the PLLA composes a continuous phase with randomly dispersed PPC domains. This kind of phase structure has a close resemblance with that formed by heating the sample to 210 °C for 5 min and then cold-crystallizing at 120 °C; compare Figure 8a with Figure 7c. When the sample is heated to 200 °C for 20 min before quenching to room temperature and then cold-crystallizing at 120 °C (Figure 8b), regular round PPC domains of tens of micrometers dispersed in continuous PLLA matrix are observed.

4. CONCLUSION

The phase structure of PLLA/PPC blends prepared under different conditions were investigated by optical microscopy. It is found that the phase structure of PLLA/PPC blends depends strongly on the blend ratio, heat-treatment temperature, and the heat-treatment time. At lower PPC content, e.g., less than 30%, the PLLA crystalline spherulites fill the whole space with the PPC dispersed in the amorphous region of PLLA. No evident phase separation has been observed under optical microscope. When the content of PPC reaches 40%, phase separation takes place. It is confirmed that phase separation of the PLLA/PPC blend happens prior to the crystallization of PLLA. Therefore, the heat-treatment temperature and time are the two most important factors that control the phase structure of the blend. At low heat-treatment temperatures, e.g., lower than 190 °C, the PPC and the amorphous PLLA part together compose a continuous matrix with the crystalline PLLA domain dispersed in it. When the sample was heat-treated at 200 °C for 5 min, a bicontinuous phase structure was observed. With further increase of the heat-treatment temperature, the crystalline PLLA composes the continuous phase with PPC domains randomly dispersed in it. Similar phase reversal phenomenon can be produced by heat-treating the samples at 200 °C for different times. Moreover, the crystallization of PLLA in the blends is influenced by the different phase separation. It is found that an increment in crystallinity is seen with increasing PPC content up to 30%. When the PPC content reaches 40%, phase separation takes place. Now the crystallinity of PLLA increases with increasing heat-treatment temperature, which leads to different phase structure.

AUTHOR INFORMATION

Corresponding Author

*E-mail: skyan@mail.buct.edu.cn. Tel.: +86-10-6445 5928. Fax: +86-10-6445 5928.

Notes

The authors declare no competing financial interest.

ACKNOWLEDGMENTS

The financial support of the National Natural Science Foundations of China (No. 50833006 and 50973008) is gratefully acknowledged.

REFERENCES

(1) Zhang, J. M.; Duan, Y. X.; Abraham, J. D.; Yukihiro, O. *Macromolecules* **2010**, *43*, 4240−4246.
(2) Lim, L. T.; Auras, R.; Rubino, M. *Prog. Polym. Sci.* **2008**, *33*, 820−852.
(3) Pan, P. J.; Inoue, Y. *Prog. Polym. Sci.* **2009**, *34*, 605−640.
(4) Zhang, J. W.; Jiang, L.; Zhu, L. Y. *Biomacromolecules* **2006**, *7*, 1551−1561.
(5) Dorgan, J. R. American Chemical Society: Washington, DC, 1999; pp 145−149.
(6) Sarvesh, K.; Agrawal, N.; Gregory, N. *Macromolecules* **2008**, *41*, 1774−1784.
(7) Pappalardo, D.; Annunziata, L.; Pellecchia, C. *Macromolecules* **2009**, *42*, 6056−6062.
(8) Li, H. Z.; Zhang, J. W. *J. Polym. Sci. Polym. Phys.* **2011**, *49*, 1051−1083.
(9) Vilay, V.; Mariatti, M.; Ahmad, Z.; Pasomsouk, K.; Todo, M. *J. Appl. Polym. Sci.* **2009**, *114*, 1784−1792.
(10) Liu, H. Z.; Chen, F.; Liu, B.; Estep, G.; Zhang, J. W. *Macromolecules* **2010**, *43*, 6058−6066.
(11) Rathi, S.; Chen, X.; Coughlin, E. B.; Hsu, S. L.; Golub, C. S.; Tzivanis, M. J. *Polymer* **2011**, *52*, 4184−4188.
(12) Breitenbach, A.; Kissel, T. *Polymer* **2000**, *41*, 4781−4792.
(13) Hsu, S. H.; Chen, W. C. *Biomaterials* **2000**, *21*, 359−367.
(14) Kimura, Y.; Matsuzaki, Y.; Yamane, J.; Kitao, T. *Polymer* **1989**, *30*, 1342−1349.
(15) Yamaoka, T.; Takahashi, Y.; Ohta, T.; Miyamoto, M.; Murakami, A.; Kimura, Y. *J. Polym. Sci., Polym. Chem.* **1999**, *37*, 1513−1522.
(16) Chen, C. C.; Chueh, J. Y.; Tseng, H.; Huang, H. M.; Lee, S. Y. *Biomaterials* **2003**, *24*, 1167−1173.
(17) Chen, G. X.; Kim, H. S.; Kim, E. S.; Yoon, J. S. *Polymer* **2005**, *46*, 11829−11836.
(18) Oksman, K.; Skrifvars, M.; Selin, J. *Compos. Sci. Technol.* **2003**, *63*, 1317−1324.
(19) An, Y.; Jiang, S.; Yan, S.; Sun, J.; Chen, X. *Chin. J. Polym. Sci.* **2011**, *29*, 513−519.
(20) Shi, X. D.; Gan, Z. H. *Eur. Polym. J.* **2007**, *43*, 4852−4858.
(21) Ma, X. F.; Yu, J. G.; Wang, N. *J. Polym. Sci. Polym. Phys.* **2006**, *44*, 94−101.
(22) Ge, X. C.; Zhu, Q.; Meng, Y. Z. *J. Appl. Polym. Sci.* **2006**, *99*, 782−787.
(23) Hirotsu, T.; Ketelaars, A. A. J.; Nakayama, K. *Polym. Degrad. Stab.* **2000**, *68*, 311−316.
(24) Li, J.; Lai, M. F.; Liu, J. J. *J. Appl. Polym. Sci.* **2004**, *92*, 2514−2521.
(25) Gagnon, D. R.; Karasz, F. E.; Thomas, E. L.; Lenz, R. W. *Synth. Met.* **1987**, *20*, 245−258.
(26) Andreatta, A.; Tokito, S.; Smith, P.; Heeger, A. J. *Mol. Cryst. Liq. Cryst.* **1990**, *189*, 169−182.
(27) Wang, J.; Li, H.; Liu, J.; Duan, Y.; Jiang, S.; Yan, S. *J. Am. Chem. Soc.* **2003**, *125*, 1496−1497.
(28) Shah, M.; Ganesan, V. *Macromolecules* **2010**, *43*, 543−552.
(29) Hou, W.; Zhou, J.; Gan, Z.; Shi, A.; Chan, C.; Li, L. *Polymer* **2007**, *48*, 4926−4931.
(30) Martin, O.; Averous, L. *Polymer* **2001**, *42*, 6209−6219.
(31) Zhang, J.; Duan, Y.; Yan, S. *Macromolecules* **2004**, *38*, 8012−8021.
(32) Zhang, J. M.; Hideto, T.; Isao, N.; Yukihiro, O. *J. Phys. Chem. B* **2004**, *108*, 11514−11520.
(33) Zhang, J. M.; Hideto, T.; Isao, N.; Yukihiro, O. *Macromolecules* **2004**, *37*, 6433−6439.
(34) De, S. J.; Kovacs, P. *Biopolymers* **1968**, *6*, 299−306.
(35) Wang, T.; Li, H.; Wang, F.; Yan, S.; Schultz, J. *J. Phys. Chem. B* **2011**, *115*, 7814−7822.
(36) Wang, T.; Li, H.; Wang, F.; Schultz, J.; Yan, S. *Polym. Chem.* **2011**, *2*, 1688−1698.
(37) Wang, T.; Li, H.; Yan, S. *Chin. J. Polym. Sci.* **2012**, *30*, 269−277.